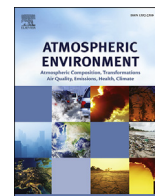




Contents lists available at ScienceDirect

Atmospheric Environment

journal homepage: www.elsevier.com/locate/atmosenv

Aerosol concentrations and composition in the North Pacific marine boundary layer



Yongjoo Choi ^a, Tae Siek Rhee ^b, Jeffrey L. Collett Jr. ^c, Taehyun Park ^a,
Seung-Myung Park ^{a,d}, Beom-Keun Seo ^a, Gyutae Park ^a, Keyhong Park ^b,
Taehyoung Lee ^{a,*}

^a Department of Environmental Science, Hankuk University of Foreign Studies, Yongin, Gyeonggi, 17035, Republic of Korea

^b Korea Polar Research Institute, Korea Institute of Ocean Science & Technology, Incheon, 21990, Republic of Korea

^c Department of Atmospheric Science, Colorado State University, Fort Collins, CO 80523, USA

^d Air Quality Research Division, National Institute of Environmental Research, Incheon 22689, Republic of Korea

HIGHLIGHTS

- Inorganic and organic aerosols, including MSA, were measured in the North Pacific marine boundary layer.
- Sulfate and organic matter were the dominant chemical species near continents.
- Biomass burning-derived oxidized organic aerosol were larger contributors near Japan.
- MSA peaked near the Sea of Okhotsk due to biological activity and utilization of nutrients during summer.
- The MSA/sulfate ratio showed a sharp gradient approach to clean marine conditions.

ARTICLE INFO

Article history:

Received 16 May 2017

Received in revised form

4 September 2017

Accepted 25 September 2017

Available online 27 September 2017

Keywords:

HR-ToF-AMS

SHIPPO

Marine aerosol

Methanesulfonic acid

Inorganic and organic aerosols

ABSTRACT

Ship-borne measurements of inorganic and organic aerosols, including methanesulfonic acid (MSA), were conducted over the Northern Pacific using a High Resolution Time of Flight Aerosol Mass Spectrometer (AMS). This study, conducted aboard the Korean ice breaker R/V Araon, was part of the SHIP-borne Pole-to-Pole Observations (SHIPPO) project. Based on air mass source region, the cruise track could be divided into five sections. Overall, the South Asia and Northern Japan ship transects showed higher aerosol concentrations due to continental pollution and biomass burning sources, respectively. In all five regions, the average mass concentrations of sulfate and organic aerosols (OA) were much higher than concentrations of nitrate and ammonium. Positive matrix factorization (PMF) analysis distinguished two organic aerosol factors as hydrocarbon-like and oxidized OA (HOA and OOA). HOA peaked in South Asia under the influence of anthropogenic pollution source areas, such as China and Korea, and generally decreased with increasing latitude across the full study region. OOA concentrations peaked in Northern Japan near the Tsugaru Strait and appear to reflect fine particle contributions from biomass burning. The mean HOA concentration in the clean marine area (Aleutian Island to Siberia) was $0.06 \mu\text{g}/\text{m}^3$ and comprised approximately 8% of the OA mass fraction. The highest MSA concentrations peaked in the Aleutian Islands at nearly $15 \mu\text{g}/\text{m}^3$, suggesting influence from higher dimethyl sulfide (DMS) emissions resulting from biological nutrient uptake during summer. The MSA/sulfate ratio, an indicator of the relative fine particle contributions of DMS and anthropogenic sources, revealed a sharp gradient as the ship approached the clean marine areas where the dominance of DMS increased. The patterns in OOA, HOA, and MSA concentrations found in this study provide a better understanding of the characteristics of inorganic and organic aerosols in the Northern Pacific Ocean.

© 2017 Elsevier Ltd. All rights reserved.

1. Introduction

Marine aerosols are an important part of naturally occurring

* Corresponding author.

E-mail address: thlee@hufs.ac.kr (T. Lee).

aerosols and exert a significant influence on the global climate (Arnold et al., 2009; Ovadnevaite et al., 2014). However, many details of the exact physical and chemical characteristics of marine aerosols are still unknown. Marine aerosols consist of both primary aerosols (e.g., sea spray) resulting from wave-breaking processes and ocean whitecap generation and secondary aerosols resulting from emission and subsequent oxidation of dimethyl sulfide (DMS) from phytoplankton, which forms sulfur-containing aerosols including non-sea-salt sulfate (nss-SO_4^{2-}) and methanesulfonic acid (MSA), or marine volatile organic compounds (VOCs) including isoprene and monoterpenes (Arnold et al., 2009; Carlton et al., 2009; Gantt and Meskhidze, 2013; Ovadnevaite et al., 2014; Russell et al., 2010; Quinn and Bates, 2011; Yassaa et al., 2008).

The principal emission source of non-sea salt sulfate (nss-SO_4^{2-}) in the marine boundary layer has been suggested to account for 25% of the global burden of nss-SO_4^{2-} (Boreddy and Kawamura, 2015). The remote marine atmosphere is influenced by transported anthropogenic nss-SO_4^{2-} and nitrate from continental sources, resulting in variation of marine background conditions (Boreddy and Kawamura, 2015). Therefore, the MSA/sulfate ratio has been a useful indicator for relative contributions of DMS and anthropogenic SO_2 sources to total sulfate levels in the marine boundary layer (Jung et al., 2014; Savoie and Prospero, 1989; Savoie et al., 2002), because MSA is produced solely from DMS (Gondwe et al., 2003).

Other inorganic and organic aerosols (OA) are often present in significant concentrations in continentally-influenced and/or clean marine conditions (Carlton et al., 2009; Middlebrook et al., 1998; Putaud et al., 2000; Shank et al., 2012). Because large amounts of OA have been observed at sites representing clean marine conditions (Middlebrook et al., 1998; Putaud et al., 2000), the possibility of an oceanic OA source of the fine mode aerosol has been investigated. Recent studies have shown that a large fraction of OA (up to 72% of mass concentration) is connected to increased biological production in the North Atlantic (O'Dowd et al., 2004; Ovadnevaite et al., 2014; Spracklen et al., 2008). Biogenic emissions, consequently, appear to be an important source of both water-soluble and insoluble OA to the marine boundary layer (Shank et al., 2012), although much remains to be learned.

Because previous studies were mainly conducted using filter sampling, it is hard to grasp the highly time-variable characteristics of aerosol in the marine boundary layer. Studies using a High Resolution Time of Flight Aerosol Mass Spectrometer (hereafter AMS) have identified new details about size-resolved temporal variations in the non-refractory marine aerosol chemical composition (Canagaratna et al., 2007; DeCarlo et al., 2006), including concentrations of nitrate, sulfate, ammonium, chloride, and organics with 5-min time resolution. In this study, an AMS was deployed from July 14–29, 2012 on board the Korean ice breaker R/V Araon travelling from Incheon, Korea to Nome, Alaska as a part of the Shipborne Pole-to-Pole Observations (SHIPPO) project to understand aerosol formation and characteristics over the Pacific Ocean (Park and Rhee, 2015). The objectives of this study were to investigate (1) the composition of aerosol in both anthropogenically impacted and remote and mostly pristine marine boundary layers, (2) the oxidation states of OA in polluted and clean marine areas, and (3) the relationships between MSA and sulfate concentrations in the marine boundary layer.

2. Methods

2.1. Ship track and identification of ship exhaust

Continuous AMS fine particle measurements were conducted on board the R/V Araon ice breaker ship, operated by the Korea Polar

Research Institute (KOPRI), sailing from Incheon (Korea) on July 13, 2012, and reaching Nome, Alaska (U.S.) on July 29, 2012 (Fig. 1 and Table 1). The data were divided into five periods (numbered from P1 to P5) depending on geographical characteristics (Table 1), which is the same sampling periods as in Park and Rhee (2015).

During the campaign, the ship's own exhaust may periodically contaminate the atmospheric measurements depending on the locations of emissions and sampling and the orientation and speed of the ship and ambient wind. A variety of criteria (e.g., wind direction, gaseous CO and CO_2 concentrations, and AMS organic fragments and/or size distributions) were used to identify and exclude contaminated data before further analysis, as discussed in detail by Park and Rhee (2015); locations of instruments in Park and Rhee (2015) and the AMS were similar except the elevation. The basic assumption of the screening procedure is that dramatic changes of CO concentrations could be an indicator of ship exhaust. Therefore, we used the following AMS data acceptance criteria to ensure stack emissions were excluded; (1) the relative wind speed must be higher than 2 knots because of effects of stack emission due to local turbulence, and (2) standard deviation of CO during 1 min should be less than 1 ppbv. Additionally, when the relative wind direction against the ship's heading was between 180° and 270° , where the ship stack was located from the air inlet, the AMS data were excluded.

2.2. Aerosol sampling

The sampling inlet was installed in the atmospheric science laboratory at the 3rd deck below the bridge, which was located on the front deck of the ship, far away from the ship exhaust (Fig. S1). Operation of the AMS has been described in detail elsewhere (e.g., Jimenez et al., 2003; Lee et al., 2015). In brief, ambient air was passed through a URG $\text{PM}_{2.5}$ cyclone at 3 LPM (URG-2000-30ED) to avoid AMS inlet clogging due to large aerosol and Perma Pure dryers (MD-110-24) maintained the relative humidity of sample air under 40%. Then, the air sample is passed through a critical orifice (100 μm pin hole) into an aerodynamic lens to cut off the aerosol size near $\sim 1 \mu\text{m}$ (DeCarlo et al., 2006). The AMS was operated in V-mode only and 5-min time resolution was used to determine the particle composition, including the concentrations of submicron nitrate, sulfate, ammonium, and organic matter. The AMS data quality is constrained by a series of calibrations and system function checks once a week, including a Micro Channel Plate (MCP) detector calibration, flow rate calibration, aerodynamic lens alignment, ionization efficiency (IE) determination, particle sizing calibration, chopper position determination, single ion determination, and voltage tuning for the mass spectrometer.

2.3. Positive matrix factorization analysis of AMS data set

The timeline of aerosol mass spectra from the AMS was analyzed using Positive Matrix Factorization (PMF) (Paatero and Tapper, 1994; Paatero, 1997). PMF analysis has been widely applied to various measurement data including speciated $\text{PM}_{2.5}$ and VOC (Baudic et al., 2016; Heo et al., 2009), and extended to apply to AMS data using the Igor Pro-based PMF evaluation tool (PET) which is also used in this study. PET deconvolves unique spectral patterns (factors) including hydrocarbon-like or oxidized aerosol from the mass spectra produced in each AMS run (Docherty et al., 2008; Lanz et al., 2007; Ulbrich et al., 2009). PMF was performed upon the V-mode AMS data after applying the error preparations outlined in SQUIRREL and PET. The method is described in greater detail elsewhere (Paatero and Tapper, 1994; Paatero, 1997; Ulbrich et al., 2009).

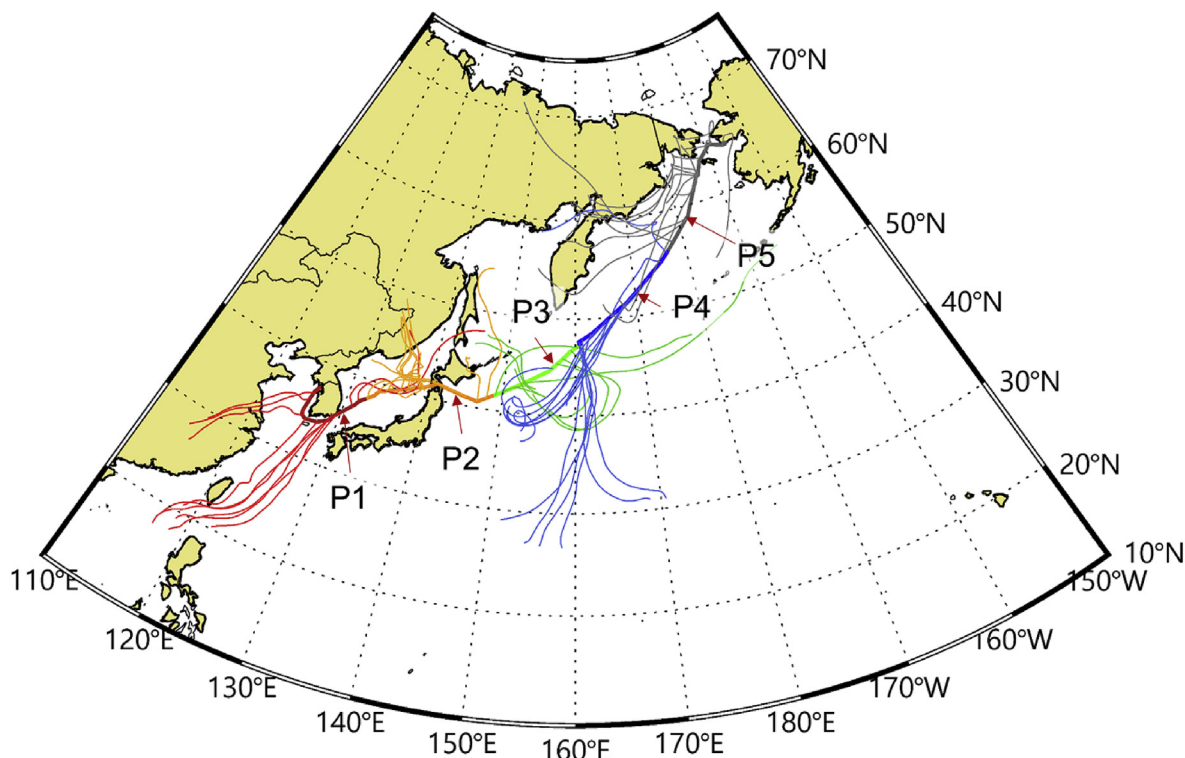


Fig. 1. Ship-track from Incheon, Korea to Nome, Alaska (13 July to 29 2012). The colored thick lines indicate ship-track sections; P1 (red); P2 (green); P3 (cyan); P4 (blue); and P5 (gray). Three-day backward trajectories of air masses computed with the HYSPLIT model for each measurement periods (P1–P5). Each line represents backward trajectories of 6-h time intervals arriving along the cruise track at 300 m above sea level. (For interpretation of the references to colour in this figure legend, the reader is referred to the web version of this article.)

Table 1

SHIPPO cruise ship track divided based on Park and Rhee (2015) which used the origin of the air masses identified by the HYSPLIT 5-day backward trajectories. Ship track sections P1 to P5 as described in Fig. 1.

Periods	Start time	End Time	Region	Description
P1	2012-07-13 18:00	2012-07-16 12:00	South Asia	Polluted - China and Korea
P2	2012-07-16 12:00	2012-07-19 6:00	Northern Japan	Polluted - Korea and Japan
P3	2012-07-19 6:00	2012-07-21 18:00	Aleutian Islands	Clean ocean with high Chlorophyll <i>a</i>
P4	2012-07-21 18:00	2012-07-25 14:00	North Pacific	Clean ocean
P5	2012-07-25 14:00	2012-07-29 20:20	Siberia	Clean ocean

3. Results and discussion

3.1. Temporal variations of aerosol concentrations

Fig. 2(a) shows the spatial variations in the concentration of major inorganic ions (ammonium, nitrate and sulfate) and organics with a variation for the latitude of the ship track during study periods P1–P5. Concentrations of non-refractory submicron particles (NR-PM₁) were highest during P1 and P2, with their mean values of 8.4 and 9.0 $\mu\text{g}/\text{m}^3$, respectively. The average concentrations during other periods (P3–P5) were decreased, ranging from 1.7 to 3.4 $\mu\text{g}/\text{m}^3$ (Table 2).

The highest NR-PM₁ concentrations were measured near the start of the ship track (P1), with a value of 46 $\mu\text{g}/\text{m}^3$ and a decrease in NR-PM₁ concentration with distance from China. Moreover, the highest sulfate concentrations were also observed during this period, up to 25 $\mu\text{g}/\text{m}^3$. These sulfate concentrations are in reasonable agreement with previously published results (up to 22 $\mu\text{g}/\text{m}^3$ for bulk aerosols) measured near Shanghai, China as reported by Chen et al. (2012). The most likely explanation for the pattern shown here is the influence of sulfur emissions from China on both PM₁ and sulfate levels in coastal areas (Chen et al., 2012;

Lee et al., 2004, 2015; Park and Rhee, 2015), consistent with transport patterns illustrated by three-day backward trajectories during P1 (see Fig. 1).

NR-PM₁ concentrations increased slightly to 22 $\mu\text{g}/\text{m}^3$ on 18 July during P2, when the ship was passing through the Tsugaru Strait (Japan). In this region, the sample was affected by biomass burning in the vicinity (Fig. 1 and S2), resulting in the highest organic aerosol concentration and fraction observed during the cruise. However, the average concentrations and fractions of inorganic aerosols, including sulfate, nitrate and ammonium, during P2 were lower than those observed in P1 (Fig. 2b and c).

When approaching the Pacific Ocean, NR-PM₁ concentrations significantly decreased below approximately 10 $\mu\text{g}/\text{m}^3$ due to influence by air masses from the clean ocean region (Fig. 1). Sulfate and OA are the dominant species in the clean ocean area and their concentrations are lower than those observed in P1 and P2 (Table 2). These concentrations are comparable to previous observations from the northwestern North Pacific and subarctic western North Pacific (Jung et al., 2014; Sasakawa and Uematsu, 2002) and from ship-borne measurements in clean marine areas (Fu et al., 2011; Gantt and Meskhidze, 2013; Quinn et al., 2004). The mean ammonium and nitrate concentrations were similarly low across

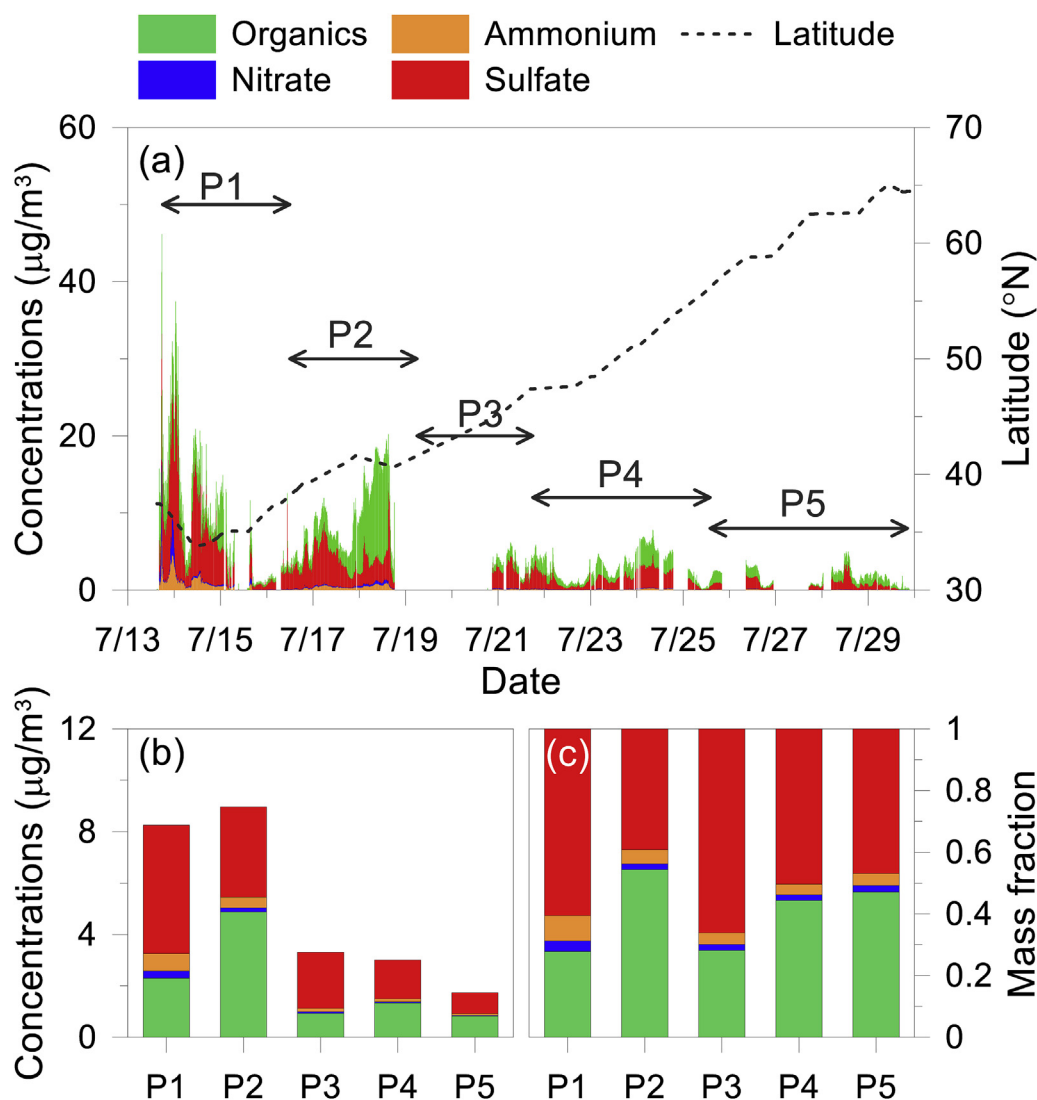


Fig. 2. (a) Temporal variation in concentrations of organic and inorganic PM₁ and latitude of the ship track during SHIPPO in 2012. (b) Mean concentrations and (c) mass fractions of the chemical measured at the ship-track section of P1 to P5.

Table 2

Mean concentrations (µg/m³) of inorganic and organic aerosols, and the mean mass fraction of each component during each ship track. Ship tracks P1 to P5 as described in Fig. 1 (Parenthesis indicated mass fraction of each species).

Periods	Nitrate	Sulfate	Ammonium	Organics	PM ₁
P1	0.25 ± 0.61 (3.00%)	5.12 ± 4.58 (61.2%)	0.7 ± 0.79 (8.36%)	2.3 ± 2.25 (27.5%)	8.36 ± 7.34
P2	0.16 ± 0.11 (1.82%)	3.52 ± 1.82 (39.3%)	0.41 ± 0.22 (4.56%)	4.87 ± 4.22 (54.3%)	8.97 ± 4.66
P3	0.06 ± 0.03 (1.85%)	2.26 ± 0.98 (66.9%)	0.13 ± 0.04 (3.71%)	0.93 ± 0.38 (27.6%)	3.38 ± 1.39
P4	0.05 ± 0.02 (1.78%)	1.39 ± 0.95 (48.4%)	0.09 ± 0.06 (3.26%)	1.33 ± 0.91 (46.6%)	2.87 ± 1.88
P5	0.03 ± 0.01 (2.03%)	0.77 ± 0.64 (45.9%)	0.06 ± 0.05 (3.64%)	0.82 ± 0.5 (48.4%)	1.68 ± 1.06
Total	0.14 ± 0.51 (2.72%)	2.68 ± 3.10 (51.0%)	0.32 ± 0.54 (6.01%)	2.12 ± 2.67 (40.3%)	5.26 ± 5.59

periods P3–P5, indicating that the NR-PM₁ consisted mainly of sulfate and OA in clean ocean areas (Quinn and Bates, 2003; Shank et al., 2012).

3.2. The evolution and oxidation degree of ambient organic aerosol

Ng et al. (2010) pointed out that m/z 44 and m/z 43 in oxidized OA (OOA) spectra consist mainly of acidic groups and non-acid oxygenates, respectively. Further, the ratio of m/z 44 to m/z 43 ($f_{44}:f_{43}$) is an indicator of the degree of oxidation of OA and a triangular region outlines the values of $f_{44}:f_{43}$ that typically indicate the range of oxidation observed in ambient OA. The relative abundances of key OA ions at m/z 44 (CO_2^-) and m/z 43 ($\text{C}_2\text{H}_3\text{O}^+$) distinguish HOA (hydrocarbon-like OA), SV-OOA (semi-volatile oxygenated OA) and LV-OOA (low volatility oxygenated OA). The HOA components show $f_{44} < 0.05$, toward the bottom of the triangular region (Fig. 3). The SV-OOA and LV-OOA components fall in the middle of the triangle and the narrow region toward the top, respectively.

In the $f_{44}:f_{43}$ diagram, the bulk of the observed OA is located in three major domains (HOA, SV-OOA and LV-OOA), indicating the various oxidation states during the ship track periods. The data for P1 (red circles) extend from HOA to LV-OOA, whereas the data for P2 are mainly located within the LV-OOA region. During period P2, the OA was slightly aged/oxidized to SV-OOA and/or LV-OOA and

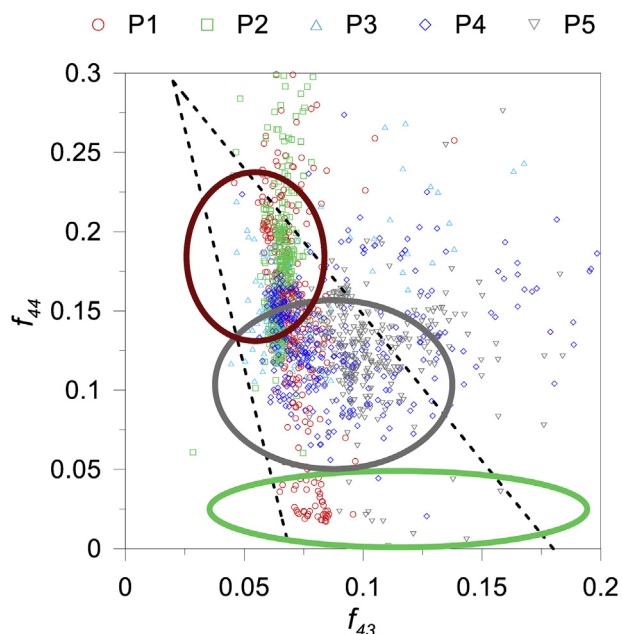


Fig. 3. Relationship between f_{44} (fraction of m/z 44 to total organic concentration) and f_{43} (same as f_{44} except for m/z 43). The triangular region is defined by two different slopes of f_{44} and f_{43} as described by Ng et al. (2010). The colors of the boundaries as ellipses are green for HOA, grey for SV-OOA and red for LV-OOA regions. (For interpretation of the references to colour in this figure legend, the reader is referred to the web version of this article.)

showed a similar pattern to previously reported results (Ng et al., 2010, 2011b; Zhang et al., 2011). The $f_{44}:f_{43}$ ratios for periods P3 to P5 shifted toward the SV-OOA domain, especially P4 and P5, indicating that SV-OOA was dominant and small amounts of HOA also existed in the clean marine area. Although P5 was classified as a clean ocean area with low PM concentrations, it is difficult to exclude the possibility that HOA is affected by air masses passing over Northeast Russia (see Fig. 1), suggesting the influence of continental anthropogenic emissions because HOA is mainly emitted from fossil fuel combustion. The van Krevelen diagram, which can help highlight bulk changes in aerosol oxygenation depending on the $\Delta H:C/\Delta O:C$ slope (Ng et al., 2011a), also indicated that OA components occupy both HOA and OOA domains during periods P1–P5 (figure not shown).

The OA can be divided into two factors, including HOA (12% of organic matter) and OOA (88% of organic matter) from the PMF analysis. The factor mass spectra for those PMF factors are shown in Fig. 4(a) and (b). The HOA component is identified by the clear hydrocarbon signature in its spectrum at m/z 41, 43, and 55 (Hildebrandt et al., 2010; Ng et al., 2010, 2011b). The OOA factor has f_{44} (CO_2) of 14% and f_{43} ($C_3H_7^+$ and $CH_3CO_3^+$) of 6%, similar to typical LV-OOA factors based on aerosol volatility ($f_{44} = 12$ –15%, $f_{43} = 5$ –7%) (e.g., Hildebrandt et al., 2010; Ng et al., 2010, 2011b; Ulbrich et al., 2009; Zhang et al., 2011). Higher HOA concentrations were measured in P1 than in other periods, likely due to influence from emissions in China and Korea (Fig. 4c and Table 3). Then HOA decreased with increasing latitude (approaching increasingly remote ocean areas), and the fraction of HOA decreased from 40% to 8%. Significant increases in OOA concentrations were observed in P2 in the area near the Tsugaru Strait, resulting from OA from biomass burning, as discussed in section 3.1 above. The mean HOA concentration in the clean ocean area (P3 to P5) was $0.06 \mu\text{g}/\text{m}^3$, with an approximately 8% mass contribution to OA. This value agrees well with observations by Decesari et al.

(2011), showing that $\leq 8\%$ of the AMS-determined organic mass is accounted for by HOA (similar to POA) in the North Atlantic boundary layer.

3.3. Temporal variation of MSA (CH_3SO_3H)

MSA, considered a characteristic component of marine secondary OA, is formed by the atmospheric reaction of DMS produced by marine biota (Wolf et al., 2015). MSA concentrations were calculated from the sulfur-containing AMS fragments of m/z 78 ($CH_2SO_2^+$), m/z 79 ($CH_3SO_2^+$) and m/z 96 ($CH_4SO_3^+$), and were scaled by a factor of 0.147 (Ge et al., 2012):

$$\text{MSA} = \frac{[\text{CH}_2\text{SO}_2^+] + [\text{CH}_3\text{SO}_2^+] + [\text{CH}_4\text{SO}_3^+]}{0.147}$$

where $CH_2SO_2^+$, $CH_3SO_2^+$, and $CH_4SO_3^+$ are the signal intensities of these three aerosol ions measured in the marine boundary layer. Previous studies have observed that the comparisons of MSA mass concentrations between AMS and PM_{10} filter measurements were varied depending on the MSA estimation methods of AMS measurement ($R^2 \geq 0.78$) (Ge et al., 2012; Huang et al., 2015, 2017; Phinney et al., 2006). This discrepancy of MSA mass concentrations between AMS and PM_{10} filter measurements can be caused from scale factors for pure MSA (e.g., 0.147 in Ge et al., 2012); however, it is hard to deduce the proper scale factor for specific measurement periods without simultaneous filter measurement.

In Fig. 5, observed MSA concentrations remained low (up to $0.19 \mu\text{g}/\text{m}^3$) from 35° N to 40° N (P1 and P2) with similar mean MSA concentrations ($0.04 \mu\text{g}/\text{m}^3$ for P1 and $0.06 \mu\text{g}/\text{m}^3$ for P2). Those values are similar to the range in MSA concentrations reported by Chen et al. (2012) and Lee et al. (2004). The MSA concentrations during P3 (clean ocean area) showed the highest concentration, reaching $0.68 \mu\text{g}/\text{m}^3$ from 45° N to 47° N, and the highest mean concentration of $0.38 \mu\text{g}/\text{m}^3$ (Fig. 5). Similarly high concentrations have also been observed in several previous studies (Chen et al., 2012; Jung et al., 2014; Savoie and Prospero, 1989). High MSA concentrations observed during P3, likely resulting from active DMS emissions from biological marine sources (e.g., phytoplankton blooms), consistent with high chlorophyll-a concentrations observed from satellite (Fig. S3), could be a major contribution in this region (Jung et al., 2014; Kim, 2015). The mean MSA concentrations during other periods (P4 to P5) decreased from 0.14 to $0.10 \mu\text{g}/\text{m}^3$ as the ship track moved to higher latitudes from 48° N to 65° N (P4 and P5).

3.4. Relationship between MSA and sulfate

The spatial and seasonal (summer maxima and winter minima) variation in the MSA/sulfate ratio over the Pacific Ocean has been characterized in previous studies, with higher ratios occurring at high latitudes (e.g., Arimoto et al., 1996; Chen et al., 2012; Saltzman et al., 1986; Savoie and Prospero, 1989).

The MSA/sulfate concentration ratio in this study varied from 0 to 0.37, with lower ratios occurring near continental regions (P1 and P2) and higher values over clean open ocean regions (P3–P5) (Fig. 5), consistent with previous studies (Chen et al., 2012; Jung et al., 2014). There were strong correlations ($R > 0.69$) between MSA concentrations and sulfate, depending on the period of the overall ship track (Fig. 6). The mean MSA/sulfate ratios for the five measurement periods were as follows: 0.011 ± 0.022 for P1, 0.016 ± 0.006 for P2, 0.161 ± 0.045 for P3, 0.091 ± 0.047 for P4 and 0.141 ± 0.075 for P5. The lowest ratio (P1) reflects the influence of air masses containing anthropogenic sulfate from nearby

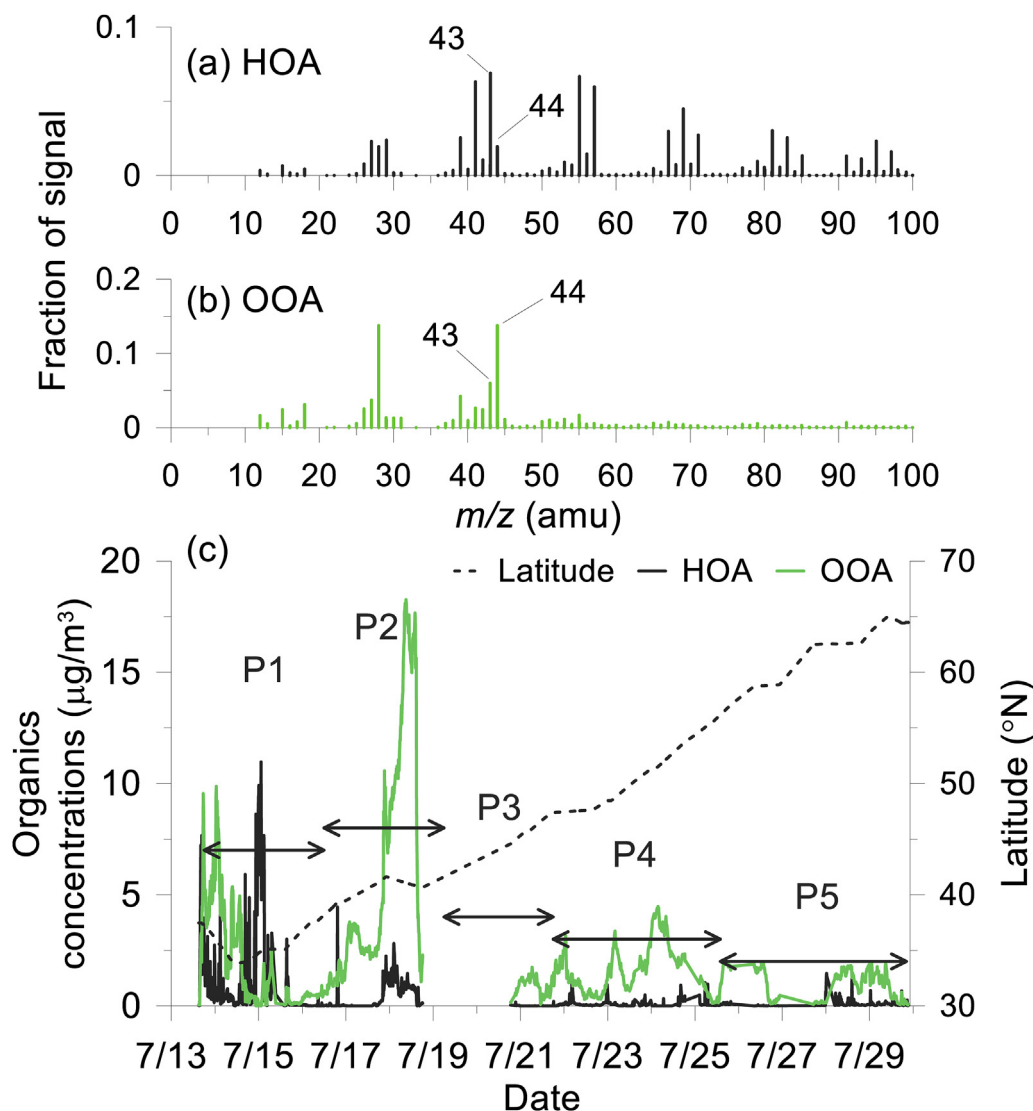


Fig. 4. Mass spectra of two OA factors consisting of (a) HOA and (b) OOA determined on the basis of PMF analysis of the HR-ToF-AMS data during SHIPPO in 2012. (c) Time series of two OA factors with ship track latitude.

Table 3

Mean concentrations ($\mu\text{g}/\text{m}^3$) of HOA and OOA in aerosols, and the mass fraction for each ship track.

Ship track	HOA		OOA	
	Mean \pm SD ^a	Mass fraction	Mean \pm SD ^a	Mass fraction
P1	1.01 \pm 2.05	40%	1.53 \pm 2.03	60%
P2	0.40 \pm 0.60	6.4%	5.80 \pm 5.38	94%
P3	0.01 \pm 0.02	0.8%	0.89 \pm 0.37	99%
P4	0.09 \pm 0.16	5.4%	1.53 \pm 1.07	95%
P5	0.09 \pm 0.16	7.9%	1.01 \pm 0.64	92%

^a Standard deviation.

continents (Chen et al., 2012), as described in 3.1. The maximum MSA/sulfate ratio was observed during P3, resulting from the elevated MSA concentrations due to enhancement of biological productivity and associated DMS production as described in 3.3. This segment also exhibited the highest correlation coefficient ($R = 0.90$), suggesting that the sulfate concentration was mainly influenced by DMS oxidation. Previous observations found MSA/sulfate ratios in the clean ocean area (P4 and P5) slightly greater

than 0.043 at Shemya (Arimoto et al., 1996) and 0.063 in the sub-arctic western north Pacific (Jung et al., 2014).

4. Summary and conclusions

We investigated spatial patterns in PM1 inorganic, organic aerosol (OA) and MSA concentrations using a High Resolution Time of Flight Aerosol Mass Spectrometer (AMS) over the Northeastern Pacific, including the East Sea and the Bering Sea. Ship tracks near South Asia (P1) and Northern Japan (P2) showed higher aerosol concentrations than other regions near clean ocean areas (P3 to P5). Continental anthropogenic pollutants dominated P1 while biomass burning-derived pollutants were larger contributors in P2. Concentrations of nitrate and ammonium were lower than concentrations of both sulfate and OA when the ship track approached open ocean areas (P3–P5). The $f_{44}:f_{43}$ ratio varied in the domains of HOA, SV-OOA, and LV-OOA, indicating the existence of various aerosol oxidation states. As the ship moved away from continental areas from P1 to P3, the portion of HOA significantly decreased, resulting in dominance by aged (oxidized) organic aerosols (SV-OOA and LV-OOA). The HOA is still present at low concentration in the clean

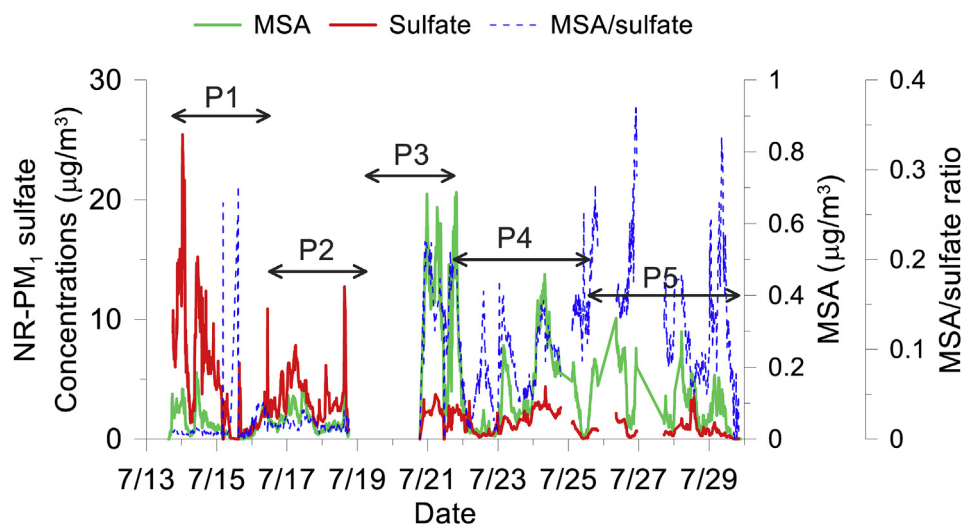


Fig. 5. Temporal changes in concentrations of MSA, sulfate and MSA/sulfate ratio with latitude of the ship track during SHIPPO in 2012.

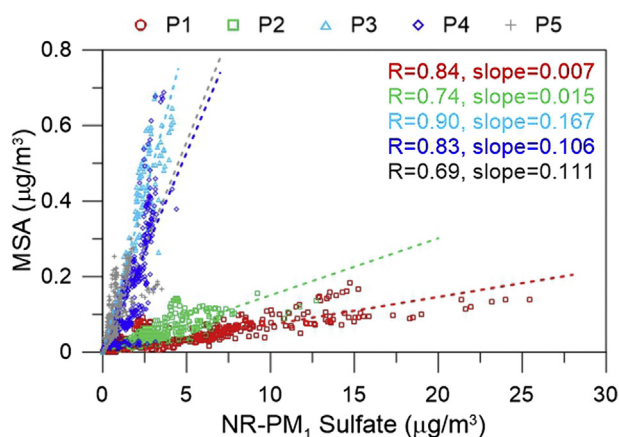


Fig. 6. Relationships between sulfate and MSA during the entire measurement period. The dashed-lines indicate the best fit lines through the origin. R and slope represent correlation coefficients and slope of best fit lines through the origin in each measurement periods.

marine areas (P3–P5). MSA concentrations remained low during P1 and P2, and the maximum concentration was found at P3, reflecting oxidation of higher DMS concentrations from intense biological activity and utilization of nutrients during summer. The MSA/sulfate ratio indicated the relative contributions of DMS and anthropogenic sources of sulfate. The MSA/sulfate ratio showed a sharp gradient when approaching clean marine conditions. Observations of the variation of organic, inorganic aerosol and MSA concentrations from SHIPPO enhance our understanding of the characteristics of polluted and clean marine areas in the Northern Pacific Ocean.

Acknowledgments

The authors thank the research scientists, captain and crew of the ice breaker R/V Araon for their on-board assistance. The field campaign was funded by the Korea Polar Research Institute (PE13410), and additional data processing and analysis was supported by a grant from the National Research Foundation of Korea (NRF-2014R1A1A1007947).

Appendix A. Supplementary data

Supplementary data related to this article can be found at <https://doi.org/10.1016/j.atmosenv.2017.09.047>.

References

- Arimoto, R., Duce, R.A., Savoie, D.L., Prospero, J.M., Talbot, R., Cullen, J.D., Tomza, U., Lewis, N.F., Ray, B.J., 1996. Relationships among aerosol constituents from Asia and the north pacific during pem-west a. *J. Geophys. Res. Atmos.* 101, 2011–2023.
- Arnold, S.R., Spracklen, D.V., Williams, J., Yassaa, N., Sciare, J., Bonsang, B., Gros, V., Peeken, I., Lewis, A.C., Alvaïn, S., Moulin, C., 2009. Evaluation of the global oceanic isoprene source and its impacts on marine organic carbon aerosol. *Atmos. Chem. Phys.* 9, 1253–1262.
- Baudic, A., Gros, V., Sauvage, S., Locoge, N., Sanchez, O., Sarda-Estève, R., Kalogridis, C., Petit, J.-E., Bonnaire, N., Baisnée, D., Favez, O., Albinet, A., Sciare, J., Bonsang, B., 2016. Seasonal variability and source apportionment of volatile organic compounds (VOCs) in the Paris megacity (France). *Atmos. Chem. Phys.* 16, 11961–11989.
- Boreddy, S.K.R., Kawamura, K., 2015. A 12-year observation of water-soluble ions in TSP aerosols collected at a remote marine location in the western North Pacific: an outflow region of Asian dust. *Atmos. Chem. Phys.* 15, 6437–6453.
- Canagaratna, M.R., Jayne, J.T., Jimenez, J.L., Allan, J.D., Alfarra, M.R., Zhang, Q., Onasch, T.B., Drewnick, F., Coe, H., Middlebrook, A., Delia, A., Williams, L.R., Trimborn, A.M., Northway, M.J., DeCarlo, P.F., Kolb, C.E., Davidovits, P., Worsnop, D.R., 2007. Chemical and microphysical characterization of ambient aerosols with the aerodyne aerosol mass spectrometer. *Mass Spectrom. Rev.* 26, 185–222.
- Carlton, A.G., Wiedinmyer, C., Kroll, J.H., 2009. A review of Secondary Organic Aerosol (SOA) formation from isoprene. *Atmos. Chem. Phys.* 9, 4987–5005.
- Chen, L., Wang, J., Gao, Y., Xu, G., Yang, X., Lin, Q., Zhang, Y., 2012. Latitudinal distributions of atmospheric MSA and MSA/nss-SO4²⁻ ratios in summer over the high latitude regions of the Southern and Northern Hemispheres. *J. Geophys. Res. Atmos.* 117 <https://doi.org/10.1029/2011JD016559>. D10306.
- DeCarlo, P.F., Kimmel, J.R., Trimborn, A., Northway, M.J., Jayne, J.T., Aiken, A.C., Gonin, M., Fuhrer, K., Horvath, T., Docherty, K.S., 2006. Field-deployable, high-resolution, time-of-flight aerosol mass spectrometer. *Anal. Chem.* 78, 8281–8289.
- Decesari, S., Finessi, E., Rinaldi, M., Paglione, M., Fuzzi, S., Stephanou, E.G., Tzias, T., Spyros, A., Ceburnis, D., O'Dowd, C., Dall'Osto, M., Harrison, R.M., Allan, J., Coe, H., Facchini, M.C., 2011. Primary and secondary marine organic aerosols over the North Atlantic Ocean during the MAP experiment. *J. Geophys. Res. Atmos.* 116 <https://doi.org/10.1029/2011JD016204>. D22210.
- Docherty, K.S., Stone, E.A., Ulbrich, I.M., DeCarlo, P.F., Snyder, D.C., Schauer, J.J., Peltier, R.E., Weber, R.J., Murphy, S.M., Seinfeld, J.H., Grover, B.D., Eatough, D.J., Jimenez, J.L., 2008. Apportionment of primary and secondary organic aerosols in southern California during the 2005 study of organic aerosols in riverside (SOAR-1). *Environ. Sci. Technol.* 42, 7655–7662.
- Fu, P., Kawamura, K., Miura, K., 2011. Molecular characterization of marine organic aerosols collected during a round-the-world cruise. *J. Geophys. Res. Atmos.* 116 <https://doi.org/10.1029/2011JD015604>. D13302.
- Gantt, B., Meskhidze, N., 2013. The physical and chemical characteristics of marine primary organic aerosol: a review. *Atmos. Chem. Phys.* 13, 3979–3996.

- Ge, X., Zhang, Q., Sun, Y., Ruehl, C.R., Setyan, A., 2012. Effect of aqueous-phase processing on aerosol chemistry and size distributions in Fresno, California, during wintertime. *Environ. Chem.* 9, 221–235.
- Gondwe, M., Krol, M., Gieskes, W., Klaassen, W., de Baar, H., 2003. The contribution of ocean-leaving DMS to the global atmospheric burdens of DMS, MSA, SO₂, and NSS SO₄²⁻. *Glob. Biogeochem. Cycles* 17, 251–25-18.
- Heo, J.B., Hopke, P.K., Yi, S.M., 2009. Source apportionment of PM_{2.5} in Seoul, Korea. *Atmos. Chem. Phys.* 9, 4957–4971.
- Hildebrandt, L., Kostenidou, E., Mihalopoulos, N., Worsnop, D.R., Donahue, N.M., Pandis, S.N., 2010. Formation of highly oxygenated organic aerosol in the atmosphere: insights from the FINOKALIA aerosol measurement experiments. *Geophys. Res. Lett.* 37, L23801.
- Huang, D.D., Li, Y.J., Lee, B.P., Chan, C.K., 2015. Analysis of organic sulfur compounds in atmospheric aerosols at the HKUST supersite in Hong Kong Using HR-ToF-AMS. *Environ. Sci. Technol.* 49, 3672–3679.
- Huang, S., Poulain, L., van Pinxteren, D., van Pinxteren, M., Wu, Z., Herrmann, H., Wiedensohler, A., 2017. Latitudinal and seasonal distribution of particulate MSA over the Atlantic using a validated quantification method with hr-tof-ams. *Environ. Sci. Technol.* 51, 418–426.
- Jimenez, J.L., Jayne, J.T., Shi, Q., Kolb, C.E., Worsnop, D.R., Yourshaw, I., Seinfeld, J.H., Flagan, R.C., Zhang, X., Smith, K.A., 2003. Ambient aerosol sampling using the aerodyne aerosol mass spectrometer, 1984–2012. *J. Geophys. Res. Atmos.* 108.
- Jung, J., Furutani, H., Uematsu, M., Park, J., 2014. Distributions of atmospheric non-sea-salt sulfate and methanesulfonic acid over the Pacific Ocean between 48°N and 55°S during summer. *Atmos. Environ.* 99, 374–384.
- Kim, G., Cho, H.-J., Seo, A., Kim, D., Gim, Y., Lee, B.Y., Yoon, Y.J., Park, K., 2015. Comparison of hygroscopicity, volatility, and mixing state of submicrometer particles between cruises over the Arctic Ocean and the Pacific Ocean. *Environ. Sci. Technol.* 49, 12024–12035.
- Lanz, V.A., Alfarra, M.R., Baltensperger, U., Buchmann, B., Hueglin, C., Prevot, A.S.H., 2007. Source apportionment of submicron organic aerosols at an urban site by factor analytical modelling of aerosol mass spectra. *Atmos. Chem. Phys.* 7, 1503–1522.
- Lee, T., Choi, J., Lee, G., Ahn, J., Park, J.S., Atwood, S.A., Schurman, M., Choi, Y., Chung, Y., Collett Jr., J.L., 2015. Characterization of aerosol composition, concentrations, and sources at Baengnyeong Island, Korea using an aerosol mass spectrometer. *Atmos. Environ.* 120, 297–306.
- Lee, G., Kahng, S.-H., Oh, J.-R., Kim, K.-R., Lee, M., 2004. Biogenic emission of dimethylsulfide from a highly eutrophicated coastal region, Masan Bay, South Korea. *Atmos. Environ.* 38, 2927–2937.
- Middlebrook, A.M., Murphy, D.M., Thomson, D.S., 1998. Observations of organic material in individual marine particles at Cape Grim during the first aerosol characterization experiment (ace 1). *J. Geophys. Res. Atmos.* 103, 16475–16483.
- Ng, N.L., Canagaratna, M.R., Jimenez, J.L., Chhabra, P.S., Seinfeld, J.H., Worsnop, D.R., 2011a. Changes in organic aerosol composition with aging inferred from aerosol mass spectra. *Atmos. Chem. Phys.* 11, 6465–6474.
- Ng, N.L., Canagaratna, M.R., Jimenez, J.L., Zhang, Q., Ulbrich, I.M., Worsnop, D.R., 2011b. Real-time methods for estimating organic component mass concentrations from aerosol mass spectrometer data. *Environ. Sci. Technol.* 45, 910–916.
- Ng, N.L., Canagaratna, M.R., Zhang, Q., Jimenez, J.L., Tian, J., Ulbrich, I.M., Kroll, J.H., Docherty, K.S., Chhabra, P.S., Bahreini, R., Murphy, S.M., Seinfeld, J.H., Hildebrandt, L., Donahue, N.M., DeCarlo, P.F., Lanz, V.A., Prévôt, A.S.H., Dinar, E., Rudich, Y., Worsnop, D.R., 2010. Organic aerosol components observed in northern hemispheric datasets from aerosol mass spectrometry. *Atmos. Chem. Phys.* 10, 4625–4641.
- O'Dowd, C.D., Facchini, M.C., Cavalli, F., Ceburnis, D., Mircea, M., Decesari, S., Fuzzi, S., Yoon, Y.J., Putaud, J.-P., 2004. Biogenically driven organic contribution to marine aerosol. *Nature* 431, 676–680.
- Ovadnevaite, J., Ceburnis, D., Leinert, S., Dall'Osto, M., Canagaratna, M., O'Doherty, S., Berresheim, H., O'Dowd, C., 2014. Submicron NE Atlantic marine aerosol chemical composition and abundance: seasonal trends and air mass categorization. *J. Geophys. Res. Atmos.* 119, 11850–11863.
- Park, K., Rhee, T.S., 2015. Source characterization of carbon monoxide and ozone over the Northwestern Pacific in summer 2012. *Atmos. Environ.* 111, 151–160.
- Paatero, P., 1997. Least squares formulation of robust non-negative factor analysis. *Chemom. Intell. Lab. Syst.* 37, 23–35.
- Paatero, P., Tapper, U., 1994. Positive matrix factorization: a non-negative factor model with optimal utilization of error estimates of data values. *Environmetrics* 5, 111–126.
- Phinney, L., Richard Leaitch, W., Lohmann, U., Boudries, H., Worsnop, D.R., Jayne, J.T., Toom-Sauntry, D., Wadleigh, M., Sharma, S., Shantz, N., 2006. Characterization of the aerosol over the sub-arctic north east Pacific Ocean. *Deep Sea Res. Part II Top. Stud. Oceanogr.* 53, 2410–2433.
- Putaud, J.P., Van Dingenen, R., Mangoni, M., Virkkula, A., Raes, F., Maring, H., Prospero, J.M., Swietlicki, E., Berg, O.H., Hillamo, R., Mäkelä, T., 2000. Chemical mass closure and assessment of the origin of the submicron aerosol in the marine boundary layer and the free troposphere at Tenerife during ACE-2. *Tellus B* 52, 141–168.
- Quinn, P.K., Bates, T.S., 2011. The case against climate regulation via oceanic phytoplankton sulphur emissions. *Nature* 480, 51–56.
- Quinn, P.K., Coffman, D.J., Bates, T.S., Welton, E.J., Covert, D.S., Miller, T.L., Johnson, J.E., Maria, S., Russell, L., Arimoto, R., Carrico, C.M., Rood, M.J., Anderson, J., 2004. Aerosol optical properties measured on board the Ronald H. Brown during ACE-Asia as a function of aerosol chemical composition and source region. *J. Geophys. Res. Atmos.* 109 <https://doi.org/10.1029/2003JD004010>. D19S01.
- Quinn, P.K., Bates, T.S., 2003. North American, Asian, and Indian haze: similar regional impacts on climate? *Geophys. Res. Lett.* 30 (11) <https://doi.org/10.1029/2003GL016934>, 1555.
- Russell, L.M., Hawkins, L.N., Frossard, A.A., Quinn, P.K., Bates, T.S., 2010. Carbohydrate-like composition of submicron atmospheric particles and their production from ocean bubble bursting. *Proc. Natl. Acad. Sci.* 107, 6652–6657.
- Saltzman, E.S., Savoie, D.L., Prospero, J.M., Zika, R.G., 1986. Methanesulfonic acid and non-sea-salt sulfate in Pacific air: regional and seasonal variations. *J. Atmos. Chem.* 4, 227–240.
- Sasakawa, M., Uematsu, M., 2002. Chemical composition of aerosol, sea fog, and rainwater in the marine boundary layer of the northwestern North Pacific and its marginal seas. *J. Geophys. Res. Atmos.* 107, ACH 17-11-ACH 17–19.
- Savoie, D.L., Arimoto, R., Keene, W.C., Prospero, J.M., Duce, R.A., Galloway, J.N., 2002. Marine biogenic and anthropogenic contributions to non-sea-salt sulfate in the marine boundary layer over the North Atlantic Ocean. *J. Geophys. Res. Atmos.* 107, AAC 3-1-AAC 3–21.
- Savoie, D.L., Prospero, J.M., 1989. Comparison of oceanic and continental sources of non-sea-salt sulphate over the Pacific Ocean. *Nature* 339, 685–687.
- Shank, L.M., Howell, S., Clarke, A.D., Freitag, S., Brekhovskikh, V., Kapustin, V., McNaughton, C., Campos, T., Wood, R., 2012. Organic matter and non-refractory aerosol over the remote Southeast Pacific: oceanic and combustion sources. *Atmos. Chem. Phys.* 12, 557–576.
- Spracklen, D.V., Arnold, S.R., Sciare, J., Carslaw, K.S., Pio, C., 2008. Globally significant oceanic source of organic carbon aerosol. *Geophys. Res. Lett.* 35 <https://doi.org/10.1029/2008GL033359>. L12811.
- Ulbrich, I.M., Canagaratna, M.R., Zhang, Q., Worsnop, D.R., Jimenez, J.L., 2009. Interpretation of organic components from Positive Matrix Factorization of aerosol mass spectrometric data. *Atmos. Chem. Phys.* 9, 2891–2918.
- Wolf, R., El Haddad, I., Crippa, M., Decesari, S., Slowik, J.G., Poulain, L., Gilardoni, S., Rinaldi, M., Carbone, S., Canonaco, F., Huang, R.J., Baltensperger, U., Prévôt, A.S.H., 2015. Marine and urban influences on summertime PM_{2.5} aerosol in the Po basin using mobile measurements. *Atmos. Environ.* 120, 447–454.
- Yassaa, N., Peeken, I., Zöllner, E., Bluhm, K., Arnold, S., Spracklen, D., Williams, J., 2008. Evidence for marine production of monoterpenes. *Environ. Chem.* 5, 391–401.
- Zhang, Q., Jimenez, J., Canagaratna, M., Ulbrich, I., Ng, N., Worsnop, D., Sun, Y., 2011. Understanding atmospheric organic aerosols via factor analysis of aerosol mass spectrometry: a review. *Anal. Bioanal. Chem.* 401, 3045–3067.